Slurry Particle Size Evolution During the Polishing of Optical Glass

Significant advances have been made in the fabrication of glass optical components since Newton's time, especially in the mechanically dominated grinding operations; however, optical polishing remains a very challenging finishing operation, primarily because of uncontrolled chemical factors and associated chemo-mechanical interactions. Most modern fabrication shops still rely on the specialized skills of experienced opticians to manage the complex system of polishing agent, fluid, glass work, and polishing tool. As an added source of difficulty, the proprietary nature of compositional data for some of the system elements (especially the glass work and polishing agent) means that knowledge of the initial process conditions is usually incomplete. Coupled with inherently low glass removal rates, the optician's labor makes polishing the most expensive operation in precision optical fabrication.

In this article, evolution of the slurry particle size distribution during aqueous glass polishing is investigated. Our primary focus is on the role of slurry fluid chemistry, which can also be influenced by the in-process dissolution of glass constituents.[1] This issue is especially significant in commercial polishing processes, where recirculation of the slurry is an economic necessity. The discussion here is limited to three glass types (Corning 7940 fused silica, Schott BK7 borosilicate crown, and Schott SF6 dense flint) and three polishing agents (CeO_2, monoclinic ZrO_2, and nanocrystalline α-Al_2O_3). A more extensive treatment of the subject, including materials of purely academic interest, may be found in Ref. 2.

Introduction

In the fabrication of typical precision optical elements, the purpose of polishing is threefold: (1) to shape the glass work to within 0.1 μm ($\lambda/5$, $\lambda = 0.5$ μm) or less of the desired surface form, (2) remove subsurface damage (SSD) created by the preceding grinding operations, and (3) reduce the peak-to-valley (PV) surface roughness to less than 5 nm ($\lambda/100$). The mechanism of glass removal, while not entirely understood, is generally accepted as plastic scratching of the hydrated or corroded glass surface by a polishing agent suspended in an aqueous fluid.[3] This mechanism is considered to be the essence of the chemo-mechanical theory of glass polishing. The most common polishing agents are CeO_2 and ZrO_2 with mean particle sizes ranging from 0.01 to 3 μm. The polishing agent is supported by a viscoelastic tool made of pitch (wood or petroleum based) or polyurethane foam. Since the polishing agent sinks into the tool until the smallest grains are load-bearing, the glass removal rate is not strongly dependent on the particle size distribution within some poorly specified upper limit.[4] The total glass thickness removed is about 25 μm, with removal rates ranging from 0.1 to 1 μm/min. The creation of SSD is not an issue in the polishing of glass because, unlike grinding, there is no fracturing of the surface.

The mechanical aspects of polishing have been modeled as an area-averaged wear process using Preston's equation[5,6]

$$\frac{dz}{dt} = C_p \frac{L}{A} \frac{ds}{dt}, \tag{1}$$

where z is the height at a point on the surface of the glass work, C_p is Preston's coefficient (units of area/force), L is the total load, A is the area over which wear occurs, and s is the path traveled by the work relative to the tool. This equation predicts that the glass removal rate at any point on the surface is proportional to the local pressure (L/A) and velocity (ds/dt). The term C_p is generally used as either a fitting parameter or an empirical measure of polishing efficiency.[7,8] The latter use is made clear by solving Eq. (1) for C_p in terms of polishing process parameters:

$$C_p = \frac{1}{\rho L} \frac{\Delta m}{\Delta s}, \tag{2}$$

where ρ is the density of the glass work, Δm is the mass lost by the glass work during a given interval of polishing time, and Δs is the total path length traveled by the tool across the work during the same time interval. Typically reported values of C_p are of the order of 10^{-14} cm^2/dyne (10^{-13} Pa^{-1} or 9.806×10^{-7} mm^2/kgf).[4,8,9]

Preston's deceivingly simple model lacks an explicit accounting of the role of process chemistry. This point is clarified by the work of Brown *et al.* on purely abrasive (i.e., chemically inactive) polishing of metals.[10] For this specific case, they proposed an expression for C_p that is proportional to the inverse of Young's modulus of the bulk metal. If glass polishing was also a purely abrasive process, then there would be no hydrated surface layer. The corresponding value of C_p, calculated using the value of Young's modulus for the bulk glass, would be of the order of 10^{-12} cm^2/dyne, which is two orders of magnitude larger than typically reported empirical values. A major portion of this discrepancy is most likely due to three chemistry-related processes: (1) the complex hydration/corrosion of multicomponent silicate glass, (2) redeposition of silica species during polishing, and (3) surface charging of the glass work and the polishing agent. Cook's review of these processes and his proposed rate model suggested a number of interesting experiments, particularly relating to the influence of surface charge on mass transport during polishing.[4] This was a precursor to the trend of increasing interest in surface charge effects in the microgrinding[11] as well as polishing[9,12,13] of optical glass.

Hunter has summarized the mechanisms for the spontaneous separation of electric charges in systems consisting of oxides and fluids.[14] The mechanisms relevant to such systems consisting of two material phases are

(a) differences in the affinity of the two phases for ions of opposite charge, and

(b) ionization of surface groups.

Mechanism (a) involves the differential adsorption of anions or cations from the fluid onto the oxide surface as well as the differential dissolution of one type of ion over another from the oxide into the fluid. Equilibrium is established when the electrochemical potential is the same in both the oxide and fluid phases for any ion that can move freely between them.

For mechanism (b), the degree of charge development (and its sign) at the fluid-oxide interface due to ionization of surface groups on the oxide depends on the pH of the fluid. Metal-oxide surfaces typically possess a high density of amphoteric hydroxyl groups that can react with either H^+ or OH^- depending on the pH:

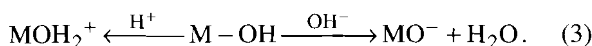

$$MOH_2^+ \xleftarrow{H^+} M-OH \xrightarrow{OH^-} MO^- + H_2O. \quad (3)$$

This behavior may be regarded as a specific example of mechanism (a), with H^+ and OH^- acting as the freely moving ions. These types of reactions can occur at the surface of a metal-oxide polishing agent particle as well as at an optical glass surface.

Well-developed techniques based on electrokinetic effects exist for measuring surface charge in systems containing either microscopic particles suspended in a fluid[15] or macroscopic solid bodies immersed in a fluid.[16] For suspended microscopic particles, measurement of the velocity of the particles under the influence of a known externally applied electric field permits the determination of the mobility of the particle. The mobility is related to the net electric charge, or surface potential, of the particle with respect to the bulk fluid. This technique is known as particle electrophoresis.

For the case of a macroscopic solid body, the surface charge can be determined by constraining the fluid to flow along a surface under the influence of a pressure gradient. Ionic charges at the surface tend to be swept along with the moving fluid, which results in an accumulation of charge downstream. The resultant potential difference induces an upstream electric current by ionic conduction through the fluid. A steady state is quickly established, and the measured potential difference along the portion of the surface over which the fluid is flowing is called the streaming potential. This streaming potential is related to both the pressure gradient driving the fluid motion and the surface potential of the solid with respect to the bulk fluid.

The above descriptions of electrokinetic measurement techniques refer to the term "surface potential." What is typically calculated from electrokinetic measurement data is known as the zeta (ζ) potential, defined as the average electric potential at the "surface of shear" near the solid (microscopic particle or macroscopic body) with respect to the bulk fluid potential. This surface of shear is an imaginary hydrodynamic boundary in the region of the fluid-solid interface. Between the solid surface and the surface of shear, the fluid is considered to be stationary in the reference frame of the solid.

Recent literature on polishing has referred to both the ζ potential[9,12] and the isoelectric point (IEP)[4] of the polishing agent and the glass work. The relationship between the IEP and the ζ potential can be readily understood in terms of the preceding discussion. The IEP of a hydrated surface is defined as the pH at which there is no net charge within the surface of shear, which clearly corresponds to $\zeta = 0$.

In spite of the complexity of the task, there has been recent progress toward the development of a deterministic glass-polishing model. Based on empirical data from two different sources, a polishing rate model has been proposed by Cook[4] that accounts for the single oxygen bond strength of the metal-oxide polishing agent (R-O, in kcal/mole), the pH of the fluid, and the IEP of the polishing agent:

$$R_c = \frac{1}{\log_{10}\left[(\mathrm{R-O}) \times |\mathrm{pH} - \mathrm{IEP}|\right]}. \quad (4)$$

The rate factor (R_c) is a predictor of the relative polishing activity of metal-oxide polishing agents.

Our earlier research with an atomic force microscope (AFM) showed that electrostatic forces between planar glass disks and individual metal-oxide polishing agent particles can be easily controlled by manipulating the pH of the surrounding fluid.[13] In this work, we investigate the manifestations of such chemically modulated forces in a planar continuous-polishing process and assess the effectiveness of manipulating the slurry chemistry to produce higher-quality surfaces in less time.

Experiment

Commercially available products were used in our experiments whenever feasible. Optical glass disks and polishing slurries were characterized in terms of the ζ potential. Slurries were further characterized in terms of the particle size distribution, and planar glass polishing experiments were conducted with a commercially compatible continuous polishing machine. Particle electrophoresis and streaming potential measurements were used to determine the IEP's of metal-oxide polishing agents and silicate glass types prior to actual polishing experiments.

1. Materials

Three glass types commonly used for precision optical components were examined in this study: Corning 7940 (fused silica),[17] Schott BK7 (borosilicate crown), and Schott SF6 (dense lead silicate flint).[18] Their chemical compositions[19,20] along with some of their fundamental properties[2,19,21] are listed in Tables 61.III and 61.IV, respectively. The action of three high-purity metal-oxide polishing agents on these three glass types was evaluated at three levels of slurry fluid pH (4, 7, and 10), spanning the range of values normally encountered in polishing. Two of the three polishing agents, Transelco CeO_2[22] and Norton monoclinic ZrO_2,[23] are supplied as aqueous slurries with a median particle size of 1 μm. The third polishing agent, Norton nanocrystalline α-Al_2O_3,[24] is also supplied as an aqueous slurry but with a median particle size of 0.6 μm. It is engineered for greater friability (i.e., a lower resistance to crumbling) than conventional α-Al_2O_3 grinding abrasives, thereby improving the prospects for successful glass polishing.[25]

Table 61.III: Composition of the three glass types (weight %).

Glass Type	SiO_2	B_2O_3	Na_2O	K_2O	BaO	PbO	As_2O_3
7940	99.9	–	–	–	–	–	–
BK7	68.9	10.1	8.8	8.4	2.8	–	1.0
SF6	26.9	–	0.5	1.0	–	71.3	0.3

The scope of our core experimental program was thus defined as the evaluation of 27 different combinations (3^3) of glass, polishing agent, and fluid.

2. Equipment and Methods

a. Preparation of glass surfaces. To ensure consistent initial conditions for each polishing experiment, a uniform planar

Table 61.IV: Some thermal and mechanical properties of the three glass types.

Glass Type	Transition Temp. (T_g) (°C)	α (10^{-6}C) (a)	Density (g/cm^3)	Young's Modulus (GPa)	H_v (kgf/mm^2)(b)	K_c (MPa m$^{1/2}$)(c)
7940	1075	0.5	2.20	73.1	953	–
BK7	559	7.1	2.51	81.0	772	0.86
SF6	423	8.1	5.18	56.0	465	0.44

(a) Linear thermal expansion coefficient (α) of 7940 determined over a temperature range of 5°C to 35°C.[9] α of BK7 and SF6 determined over a range of –30°C to 70°C.[21]
(b) Vickers hardness (H_v) measured using 0.05 kgf with samples immersed in water.[2]
(c) Fracture toughness (K_c) also measured using 0.05 kgf with samples immersed in water.[2] K_c is undefined here for fused silica because it does not fracture radially under such a low load.

disk geometry was adopted for all glass samples. Fine annealed plates were rough ground to a thickness of 15 mm and then core drilled to produce at least two dozen 40-mm-diam disks of each glass type. The individual disks were beveled and then processed using a controlled grinding strategy to minimize the depth of subsurface damage (SSD).[26] A cast iron tool and Microgrit #9 Al_2O_3 abrasive,[27] which has a median particle size of 5.75 μm, were used in the last fine-grinding operation. The resultant PV surface roughness was measured over a 4-mm scan length using a Pocket Surf III roughness gage,[28] and the depth of SSD was measured using a modification of the Itek ball method.[29] All surface sampling measurements, including PV roughness and SSD, were taken at five sites per disk: the center site plus the four sites within 5 mm of the edge at the 3, 6, 9, and 12 o'clock positions.

b. ζ potential and particle-size analysis. The ζ potential values of the three optical glass types were determined using a Brookhaven EKA electrokinetic analyzer.[30] Six disks of each glass type were cut and rough ground to the rectangular dimensions (33 × 20 × 5 mm) required to line the fluid cell of the Brookhaven EKA. One large face of each rectangular sample was fine ground as specified above and then polished using a pitch tool with an aqueous slurry of monoclinic ZrO_2. The polished surfaces were planar to within $\lambda/2$ with a scratch/dig quality of 60/40.[31] Samples of a given glass type were cleaned and mounted end-to-end in the upper and lower recesses of the EKA streaming potential cell with the polished surfaces exposed to the fluid. The streaming potential that developed along the surface of the glass-lined channel was measured while an electrolyte solution (1×10^{-3} M aqueous KCl) was forced, by external pressure, to flow along the surface. The pH values were varied between 3 and 10 by adding either HCl or NaOH to the transport electrolyte. The ζ potential values, calculated from the streaming potential measurements using the Briggs method,[15,16] were plotted as a function of fluid pH. The corresponding IEP values of each glass type (pH at which $\zeta = 0$) were obtained by interpolation.

The ζ potential values of the three polishing agents were determined using a Brookhaven ZetaPlus zeta potential analyzer,[32] which measures the electrokinetic mobility of particles suspended in a fluid using electrophoretic light scattering (ELS). The ζ potential, calculated from the electrokinetic mobility using the Smoluchowski equation,[15] was measured with the polishing agents suspended in water as well as in aqueous solutions of NaCl and catechol (1,2-$(HO)_2C_6H_4$). Catechol was chosen as a fluid additive because of its reported role as a potential silica sequestering agent during polishing with pitch tools.[4,9,33] Since a salt-rich, aqueous environment is known to effectively screen out electrostatic interactions near macroscopic oxide surfaces[34] and between particles in colloidal systems,[35,36] NaCl was also chosen as a fluid additive. Samples of each of the three slurries as received from the manufacturers were diluted (10:1) with three different carrier fluids: deionized water, aqueous catechol (500 ppm, 4.5×10^{-3} M), and aqueous NaCl [500 ppm, (0.01 M)]. The catechol concentration was chosen based on the maximum conceivable evolution of analogous compounds from a pitch polishing tool in recirculated slurry systems.[37] The maximum salt concentration was limited by the electrolytic current handling capability of the ZetaPlus instrument. Small working volumes of the nine polishing agent/fluid combinations were prepared at three pH values (4, 7, and 10) adjusted by the addition of HCl or NaOH. Measured ζ potential values of each polishing agent/fluid combination were then plotted as a function of pH, and the corresponding IEP values were obtained by interpolation.

The particle size distribution of polishing slurries was measured using a Horiba LA900.[38] This instrument optically determines the size of particles suspended in a fluid over a range of 0.04 to 1000 μm by combining Fraunhofer diffraction and Mie scattering information.[39] Typically, two or three droplets of a given slurry were dispersed directly into the carrier fluid ($V \approx 250$ ml) of the LA900. An aqueous solution of an anionic surfactant [$(NaPO_3)_6$, 0.2% by weight] was used as the carrier fluid to prevent any agglomeration of the suspended metal-oxide particles. The diluted slurry was recirculated through the LA900 until the forward-scattered red light ($\lambda = 633$ nm) signal stabilized, indicating uniform mixing. The particle size distribution was then measured and stored as a 74-bin histogram.

c. Glass polishing experiments. Glass polishing experiments were conducted on a custom-built, 535-mm-diam continuous polishing machine (CPM) with a 297-mm-diam conditioner and a pair of 178-mm-diam work rings (for individual work pieces). The theory and operational considerations of this planar polishing machine have been presented elsewhere by Preston[5] and Cooke *et al.*[40] and will not be discussed here. Unique features of our CPM include a vacuum-activated slurry agitation/recirculation system,[11] a mechanical agitator in the outer catchment trough to prevent liquid/solid separation by settling, and *in situ* measurement of the frictional force (F_T) between the polishing tool and an individual 40-mm-diam glass work piece using an Entran load cell.[41] The overall sensitivity of the frictional force measurement system is approximately ±0.1 N.

Given the ambitiously large number of material combinations to be evaluated and the need to eliminate any chemical carryover between experiments, polyurethane foam was used instead of pitch as the polishing tool. Although this choice simplifies tool replacement between experiments, the surface figure of the work, or edge roll-off, was compromised. On the basis of cost and the availability of die-cut sheets large enough to cover the 535-mm-diam turntable of our CPM, we selected a 0.5-mm-thick blown polyurethane pad, Rodel HSP.[42] The open cellular structure of this material provides a high density of sites for retaining polishing agent particles, which is a necessary condition for efficient glass removal during polishing with any polyurethane tool.[43]

The primary role of the CPM conditioner in our polishing experiments was to dominate the process chemistry by providing a significant surface area for tool/slurry/glass interactions. The conditioner also functioned as a truing device by shearing off any local asperities on the surface of the polyurethane tool.[44] To isolate glass-specific chemical effects, a separate conditioner was prepared for each of the three glass types that were polished. Each conditioner was fabricated by blocking 17 individual glass disks (40-mm diam, 15 mm thick) to a large Pyrex disk (297-mm diam, 25 mm thick). Since the functional surface of the conditioner was made of the same glass type as the individual work piece in the frictional force measurement system, only the particular glass type being studied in a given experiment participated in the process chemistry. This choice of common glass types essentially eliminated any competing effects that could be attributed to a different conditioner material.

A consistent CPM operational procedure was followed in each of the glass polishing experiments. Since chemistry-related issues were our primary concern, constant values of pressure (40 gf/cm^2) and synchronous rotation rate (9 RPM for the turntable and work rings) were maintained throughout the experiments.

At the conclusion of each experiment, the roughness of a blocked disk near the center of the conditioner was measured using a Zygo Maxim-3D laser interference microscope.[45] The surface figure of the glass work and the conditioner disk was evaluated using a Davidson Optronics Fizeau interferometer, which has a He-Ne laser source ($\lambda = 632.8$ nm) and a 127-mm-diam reference flat for testing planar surfaces.[46]

The glass removal rate ($\Delta z/\Delta t$) was calculated from the mass loss (Δm) of the glass work over a given time interval (Δt) using[11]

$$\frac{\Delta z}{\Delta t} = \frac{1}{\rho A}\frac{\Delta m}{\Delta t}, \tag{5}$$

where ρ is the glass density and A is the area of the work in contact with the polyurethane pad. The mass loss was determined by weighing the work before and after polishing using an analytical balance with a reproducibility (one standard deviation) of 20 μg. The maximum uncertainty in the reported glass removal rates was 3%.

A typical polishing experiment required approximately 7 h, including cleanup time. The polyurethane pad was replaced whenever an experiment called for a change in glass type or polishing agent. New pads were preconditioned by an 8-h polishing session with the slurry and glass type of interest, which ensured that the pad was fully charged with polishing agent particles.

Results and Discussion

1. Glass Surface Conditions prior to Polishing

The surface conditions of each glass type following fine grinding with #9 Al_2O_3 abrasive are summarized in Table 61.V in terms of the PV roughness and depth of SSD. The results clearly demonstrate that the performance of a given loose abrasive grinding operation is highly dependent on the glass type. From Table 61.V, we see that only 7940 follows the constant SSD-to-PV roughness ratio of 4.0 (±0.4) for loose abrasive grinding advanced by Aleinikov.[47] The two multi-component glass types, BK7 and SF6, have significantly lower SSD-to-PV roughness ratios.

Table 61.V: Roughness and subsurface damage of the three glass types after fine grinding with #9 Al_2O_3 abrasive.

Glass Type	PV Roughness (μm) (average of five sites)	Standard Deviation (μm)	SSD Depth (μm) (average of five sites)	Standard Deviation (μm)
7940	2.2	0.3	8.1	0.6
BK7	2.4	0.5	5.3	0.4
SF6	4.2	0.7	4.0	0.2

2. Isoelectric Point (IEP) Values of Optical Glasses and Polishing Agents

The pH dependence of the ζ potential values obtained for each glass type using the Brookhaven EKA instrument is

shown in Fig. 61.21. The corresponding IEP values of each glass type, obtained by interpolation, are listed in the legend.

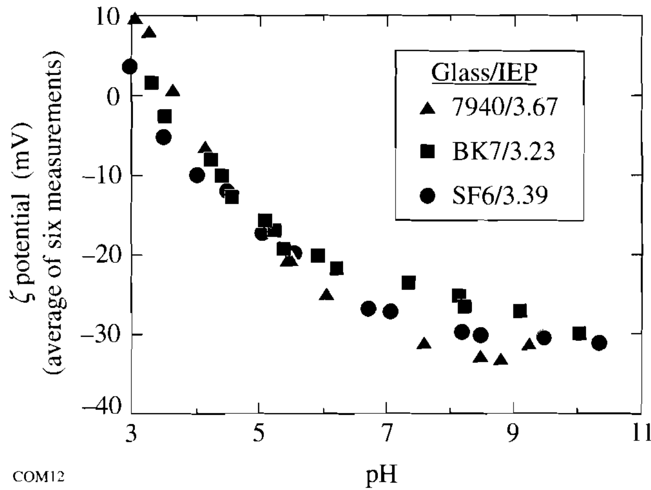

Figure 61.21
Zeta potential of 7940, BK7, and SF6 versus fluid pH. The pH was adjusted by the addition of HCl or NaOH to the transport fluid (1×10^{-3} M aqueous KCl). Error bars $\leq \pm 2$ mV (± 3 standard deviations) have been omitted for clarity.

Several important observations can be made concerning the results shown in Fig. 61.21:

- The measured value of the IEP of 7940 is in excellent agreement with that reported by Jednacak *et al.* for vitreous silica.[48]

- The ζ potential values of the three glass types are all negative (i.e., the surfaces are negatively charged due to the dissociation of OH groups) for the entire range of pH values usually encountered in optical polishing ($4 \leq \text{pH} \leq 10$).

- While the presence of significant amounts of intermediates and/or modifiers in BK7 and SF6 results in only a modest reduction of their IEP values relative to that of 7940, the ζ potential values are fairly distinctive for pH values between 6 and 9. This behavior is caused by differences in the density and charging characteristics of active surface oxide species, ostensibly due to the compositional differences between the three glass types.

The ζ potential values of each polishing agent were measured in all nine combinations of fluid additive and pH using the Brookhaven ZetaPlus instrument. The results for each polishing agent/fluid combination, when plotted as a function of pH, allowed us to determine the IEP values by interpolation, as shown for nanocrystalline Al_2O_3 suspended in aqueous catechol in Fig. 61.22. The IEP values for the eight remaining combinations of polishing agent and fluid additive were obtained by similar means and are summarized in Table 61.VI. The IEP values published by Cook[4] are also included in the table for reference.

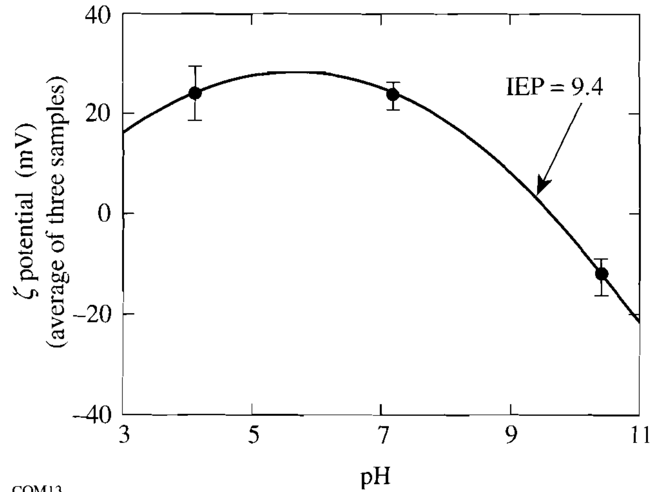

Figure 61.22
Zeta potential of the nanocrystalline Al_2O_3 polishing agent diluted in aqueous catechol (500 ppm, 4.5×10^{-3} M) versus fluid pH. The pH was adjusted by the addition of HCl or NaOH to the fluid. The data shown represents an average of three samples with ± 1 standard deviation error bars.

A remarkable feature of the data in Table 61.VI is the consistency between the measured and previously published IEP values for nanocrystalline Al_2O_3, which is an indication of the lack of specifically adsorbed ions on the surface of the polishing agent.[49] Conversely, the IEP values of CeO_2 and ZrO_2 are very sensitive to the fluid chemistry. The presence of either additive reduces the IEP values of both polishing agents, which suggests that catechol and NaCl provide ions that are specifically adsorbed at the surfaces of CeO_2 and ZrO_2. These results are considered valid only in the absence of mechanical action since individual polishing agent particles are not subjected to mechanical forces that might cause them to crumble during ζ potential measurements. The total active surface area of the polishing agent particles also remains essentially constant, unlike the case when glass is polished.

3. Original Particle Size Distribution and Friability of the Polishing Agents

The original particle size distribution of each slurry as re-

Table 61.VI Isoelectric point (IEP) values of the three polishing agents in deionized water, aqueous catechol, and aqueous sodium chloride.

Polishing Agent	IEP previously published (Ref. 4)	IEP measured in deionized water	IEP measured in catechol (aq) (4.5×10^{-3} M) (500 ppm)	IEP measured in NaCl (aq) (1.0×10^{-2} M) (584 ppm)
CeO_2	6.8	8.8	7.0	7.3
m-ZrO_2	6.2	6.3	3.0	5.0
n-Al_2O_3	9.5	9.3	9.4	9.3

ceived from the manufacturers was measured using the Horiba LA900 instrument. All three polishing agents fall within the median particle size range of 0.01 to 3.0 μm that is typical of precision polishing operations, as shown in Table 61.VII.

Table 61.VII Original particle size statistics of the three polishing agents.

Polishing Agent	Median Size (μm)	Maximum Size (μm)	Minimum Size (μm)
CeO_2	1.00	4.47	0.23
m-ZrO_2	1.34	5.12	0.23
n-Al_2O_3	0.59	5.12	0.26

The friability of each polishing agent was assessed by evaluating particle size distribution in recirculated slurry samples exposed to 20-kHz, 40-W ultrasound in the LA 900 instrument. These measurements were conducted between successive, 3-min exposures to ultrasound.

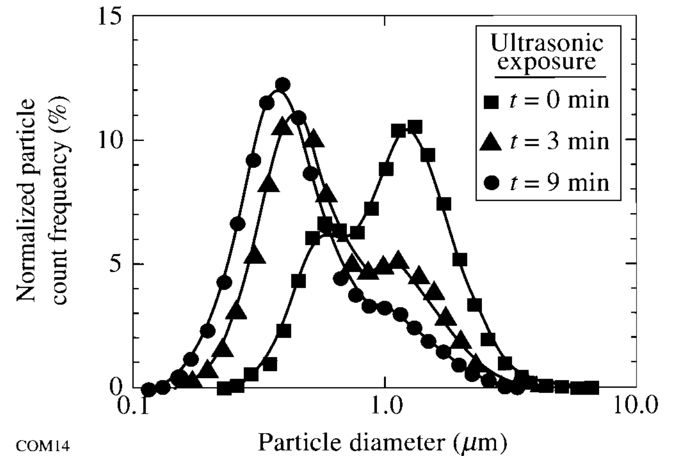

Figure 61.23
Effect of ultrasonic energy on the particle size distribution of the CeO_2 slurry. Particle size measurements were performed between successive 3-min exposures to ultrasound (40 W, 20 kHz). For clarity, the $t = 6$ min. distribution has been omitted.

Figure 61.23 illustrates the effect of ultrasonic energy on the particle size distribution of CeO_2. The initial distribution (t = 0 min) is bimodal, with the dominant mode representing the larger particles in the population. After 3 min of ultrasonic exposure, the distribution character is reversed, with the dominant mode representing the smaller particles in the population. Evidently, the ultrasonic energy induced a significant fraction of the CeO_2 particles to break apart. After 6 min (not shown) and 9 min of ultrasonic vibration, the size distribution shifts further toward smaller particle diameters, but not as dramatically as within the first 3 min.

The effect of ultrasonic energy on the median particle size of all three polishing agents is shown in Fig. 61.24. Based on the decaying exponential character of the size dependence shown in the figure, we can define an empirical ultrasonic friability index F_{us} as

$$F_{us} = -\frac{1}{U} \ln\left(\frac{D}{D_0}\right), \tag{6}$$

where D is the median particle size measured after exposure to ultrasonic energy U and D_0 is the original median particle size. This friability index F_{us} is a useful measure of the relative change in median particle size per unit of ultrasonic energy, i.e., the more friable the polishing agent, the larger the value of F_{us}.

The median particle size and corresponding value of F_{us} for all three polishing agents after 3 and 6 min of ultrasonic exposure are listed in Table 61.VIII. The original median particle size ($t = 0$) is also given in Table 61.VIII for convenient reference. In terms of F_{us}, nanocrystalline Al_2O_3 is the most friable polishing agent, followed in decreasing order by CeO_2 and monoclinic ZrO_2.

Table 61.VIII: Median particle size and ultrasonic friability index of the three polishing agents.

Polishing Agent	Median Size (μm) (t = 0 min)	Median Size (μm) (t = 3 min)	F_{us} (t = 3 min) ($\times 10^{-5}$/J)	Median Size (μm) (t = 6 min)	F_{us} (t = 6 min) ($\times 10^{-5}$/J)
CeO_2	1.00	0.50	9.6	0.43	5.9
m-ZrO_2	1.34	0.89	5.7	0.87	3.0
n-Al_2O_3	0.59	0.29	9.9	0.21	7.2

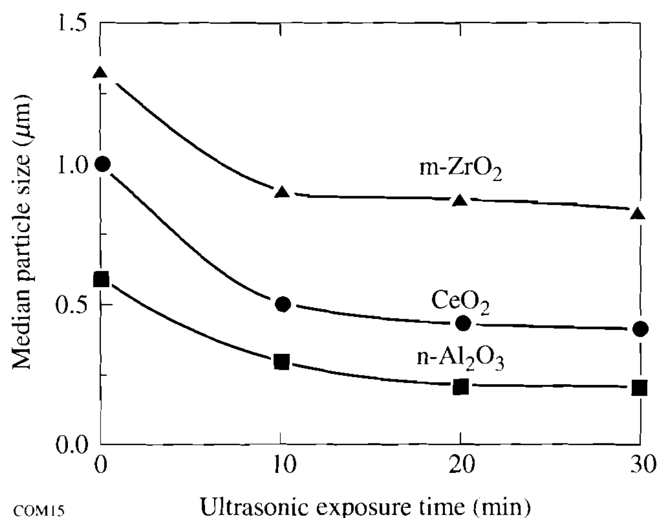

Figure 61.24
Effect of ultrasonic exposure time on the median particle size of the polishing agents.

4. Glass Polishing Experiments

Two preliminary experiments with the CPM were conducted using the most commercially important glass and polishing agents, BK7 and CeO_2, respectively. The goals of these experiments were

- to assess the in-process evolution of slurry particle size over a prolonged period of polishing, and
- to study the effect of catechol and NaCl as slurry additives.

The core experiments were then conducted using all 27 combinations of polishing agent, glass type, and slurry fluid pH. The results of each experiment are discussed below.

a. Assessment of in-process particle size evolution. The effective working lifetime of the polyurethane pad and slurry was initially determined by running the CPM with a new pad, a BK7 work and conditioner, and a fresh batch of CeO_2 slurry at pH 7 for 30 consecutive hours. The mass loss of the work and the slurry particle size distribution were measured hourly for the first 8 h, then at 15- and 30-h intervals.

The resulting glass removal rate and median particle size are plotted versus polishing time in Fig. 61.25. The glass removal rate is seen to stabilize after 6 h, which validates the need to condition new pads for at least this length of time. Between 8 and 30 h of polishing, the glass removal rate is essentially constant. This experiment established a reasonable minimum pad lifetime of 30 h, which was never exceeded during the remaining CPM experiments.

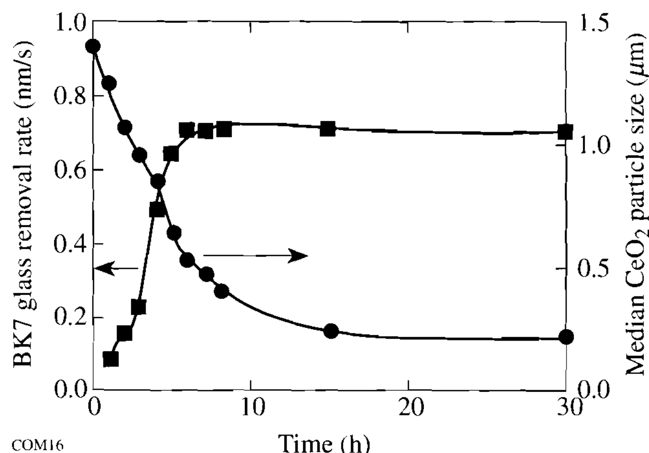

Figure 61.25
Removal rate of BK7 and the corresponding median size of the CeO_2 polishing agent versus polishing time.

After 6 h of polishing, the median CeO_2 particle size was reduced to 0.64 μm (approximately 50% of the initial value). Comparison of Figs. 61.24 and 61.25 suggests an equivalence relationship between 6 h of BK7 polishing under these conditions with 3 min of ultrasonic vibration in the Horiba LA900. These results also serve as a reminder that the glass polishing process also functions as a milling process for the polishing agent.

b. Effect of catechol and sodium chloride as slurry additives. Our earlier AFM screening experiments[13] revealed that catechol and NaCl function only to buffer mildly the forces between individual metal-oxide particles and polished glass surfaces. Their strong influence on the measured IEP values of CeO_2 and ZrO_2, as indicated in Table 61.IV, suggests the possibility of more-complex interactions between slurry particles. To resolve this issue, we studied the effect of catechol and NaCl as slurry additives using the CPM.

The average BK7 glass removal rate obtained during 4 h of polishing with aqueous CeO_2 slurries containing no slurry fluid additive, aqueous catechol (500 ppm, 4.5×10^{-3} M), and NaCl (5% by weight, 0.86 M) is plotted as a function of slurry pH in Fig. 61.26. At each of the three pH levels, the relative effect of the additives on the glass removal rate was quite consistent. The additive-free slurry fluid yielded the maximum removal rate, followed by aqueous catechol and aqueous NaCl. The maximum removal rate was obtained with no additive at pH 7. In contrast with the glass removal rate, the final rms surface roughness values (average of five measurements) of the conditioner for all nine combinations of slurry fluid additive and pH were nearly indistinguishable, averaging from only 10 to 16 Å.

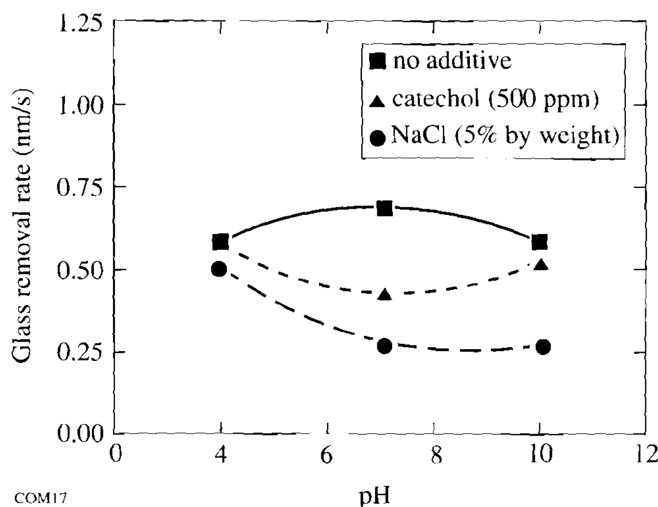

Figure 61.26
Glass removal rate as a function of slurry pH and slurry additive for polishing of BK7 with CeO_2.

These results demonstrate that, in terms of final BK7 surface roughness, the performance of CeO_2 is insensitive to significant variations in fluid chemistry. This insensitivity to fluid chemistry variations implies that an insignificant level of specifically adsorbed ions evolve from BK7 glass during the polishing process. There also is a penalty for using either catechol or NaCl as a slurry additive between pH 4 and pH 10, as evidenced by the lower glass removal rate. Since these additives made no significant impact on the polishing process, they were excluded from the remaining experiments.

c. Core glass polishing experiments. The results of the 27 core polishing experiments with CeO_2, monoclinic ZrO_2, and nanocrystalline Al_2O_3 are summarized in Table 61.IX. The range of data presented includes the average glass removal rate (RR) during each 4-h polishing session, the corresponding value of Preston's coefficient (C_p), the coefficient of friction (μ) between the work and the polyurethane pad, the final rms surface roughness of the conditioner, and the ratio of the final and original median particle size (D_f/D_0) of the slurry.

A careful review of Table 61.IX shows that polishing slurries containing monoclinic ZrO_2 are clearly the least sensitive to glass type or slurry pH, while those containing nanocrystalline Al_2O_3 are the most sensitive to these chemistry-related process factors. The CeO_2 results are intermediate to the other two polishing agents. This ordering of chemical sensitivity is identical to the ultrasonic friability index ordering (Table 61.VIII) but is contrary to the IEP stability (Table 61.VI). This apparent inconsistency can be reconciled if the available surface area of the polishing agent is taken into account. From Eq. (3), the total number of hydroxyl groups able to participate in ionization reactions scales with the combined surface area of the polishing agent particles in the recirculated slurry. Highly friable polishing agent particles will crumble progressively with use, exposing new active surface groups and accentuating the chemical aspect of their performance.

The coefficient of friction (μ) has been shown previously to be a good quantitative indicator of the efficiency of glass removal[9,12] and, as such, is a useful element with which to begin quantitative interpretation of the data in Table 61.IX. In Fig. 61.27, C_p is plotted as a function of μ for all 27 core polishing experiments. Although there are a number of outlying points, the reasonably good linear correlation ($r^2 = 0.718$) confirms quantitatively that μ may be regarded as a measure of the useful mechanical work done during polishing. Those process conditions that induced a value of μ in excess of 0.4 always resulted in a value of C_p characteristic of efficient mass transport away from the work ($\geq 10^{-13}$ cm^2/dyne).

If one studies the effect of slurry pH on the efficiency of glass removal, an interesting pattern emerges from the data.

Table 61.IX: Results of the core polishing experiments.

Polishing Agent	Glass Type	Slurry pH	RR (nm/s)	C_p ($\times 10^{-14}$ cm^2/dyne)	Friction Coefficient (μ)	rms Roughness (Å)	D_f/D_0
CeO_2	7940	4	0.141	2.2	0.27	13	1.22
"	"	7	0.215	3.3	0.31	12	1.11
"	"	10	0.200	3.1	0.30	10	0.61
"	BK7	4	0.582	8.9	0.32	16	2.36
"	"	7	0.680	10.4	0.41	13	0.55
"	"	10	0.580	8.8	0.29	11	0.25
"	SF6	4	0.270	4.1	0.32	478	1.78
"	"	7	0.104	1.6	0.28	308	0.37
"	"	10	0.788	12.0	0.48	13	0.51
m-ZrO_2	7940	4	0.307	4.7	0.35	13	0.85
"	"	7	0.241	3.7	0.35	12	0.20
"	"	10	0.253	3.8	0.33	13	0.47
"	BK7	4	0.673	10.3	0.38	19	2.15
"	"	7	0.530	8.1	0.40	16	0.80
"	"	10	0.524	8.0	0.37	14	0.62
"	SF6	4	1.110	16.9	0.49	24	1.36
"	"	7	0.733	11.2	0.48	21	0.83
"	"	10	0.778	11.8	0.48	14	0.76
n-Al_2O_3	7940	4	0.123	1.9	0.28	243	0.54
"	"	7	0.033	0.5	0.25	167	3.92
"	"	10	0.147	2.2	0.31	16	0.56
"	BK7	4	0.353	5.4	0.32	24	0.64
"	"	7	0.029	0.4	0.24	66	3.75
"	"	10	0.364	5.5	0.29	10	0.29
"	SF6	4	0.713	10.9	0.38	19	0.80
"	"	7	0.077	1.2	0.34	609	4.00
"	"	10	0.966	14.7	0.41	12	0.56

Except for the case of CeO_2 and SF6, a glass prone to selective corrosion of the PbO network modifier in acidic to neutral fluids,[50] each polishing agent exhibits a unique, glass-independent optimum pH for the maximum removal rate. For CeO_2, monoclinic ZrO_2, and nanocrystalline Al_2O_3, the glass removal rates were maximized at pH 7, 4, and 10, respectively. Returning to Table 61.VI, these optimum pH values roughly correspond to the respective IEP values measured in the presence of specifically adsorbed ions (i.e., in 0.01-M aqueous NaCl). An abundance of such ions was assumed to be present during our polishing experiments because of the dissolution of glass constituents and the use of HCl or NaOH to adjust the slurry pH. Given this assumption, our results are partially consistent with Cook's rate model, which predicts a maximum glass removal rate for a given polishing agent if the slurry pH is close to the IEP of the polishing agent [Eq. (4)]. However, as shown in Figs. 61.28–61.31, the reliability of the rate constant (R_c) as a predictor of glass removal rates is suspect. This reliability issue is especially apparent in Figs. 61.30 and 61.31, which show that R_c is not positively correlated with removal rates obtained in fluids that are corrosive to the glass.

The optimum pH for maximum glass removal did not result necessarily in the smoothest possible surfaces, which is a primary objective of polishing. Minimum surface roughness values for all nine combinations of polishing agent and glass

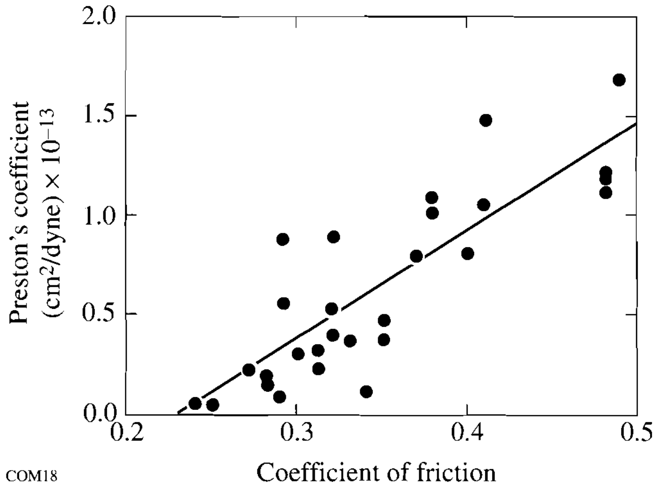

Figure 61.27
Preston's coefficient versus the coefficient of friction between the glass work and the polyurethane pad.

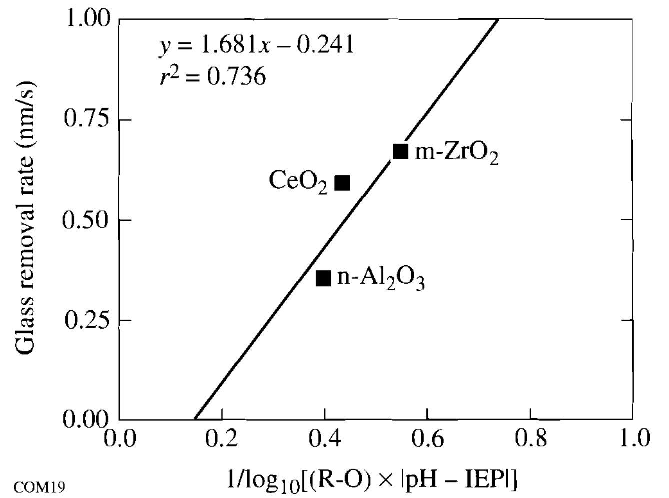

Figure 61.28
Glass removal rate versus the rate constant [4] for BK7 polishing at pH 4. (R-O) is the single oxygen bond strength (units of kcal/mole) of the polishing agent.

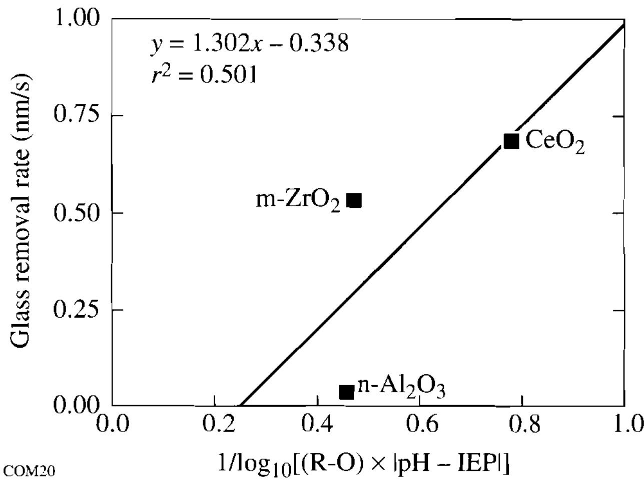

Figure 61.29
Glass removal rate versus the rate constant [4] for BK7 polishing at pH 7. (R-O) is the single oxygen bond strength (units of kcal/mole) of the polishing agent.

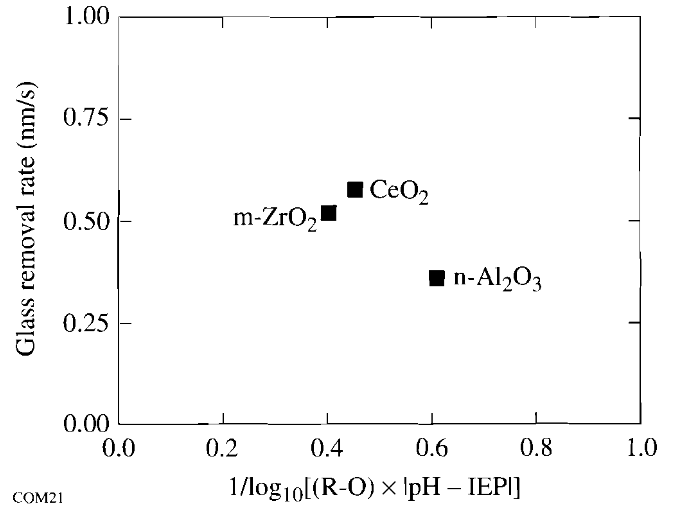

Figure 61.30
Glass removal rate versus the rate constant [4] for BK7 polishing at pH 10. (R-O) is the single oxygen bond strength (units of kcal/mole) of the polishing agent.

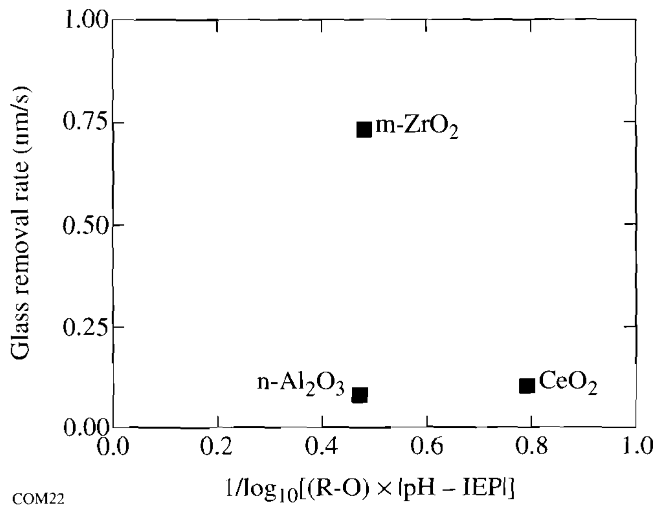

Figure 61.31
Glass removal rate versus the rate constant [4] for SF6 polishing at pH 7. (R-O) is the single oxygen bond strength (units of kcal/mole) of the polishing agent.

type were obtained when the slurry was maintained at pH 10. To understand this result, it should first be noted that all three polishing agents and all three glass types have a negative surface charge density at pH 10. As indicated by D_f/D_0, significant in-process reduction of the mean slurry particle size occurred for all nine combinations of polishing agent and glass type at this pH level. The repulsive electrostatic interparticle forces induced by the basic fluid environment inhibit the formation of agglomerates in the slurry, thereby preventing the formation of deep scratches or sleeks on the surface of the glass work. The aqueous solubility of silica, which forms the network of all three glass types, is also sharply accelerated above pH 8.[51] At pH 10, it is therefore quite plausible to expect preferential dissolution of any microscopic irregularities on the silicate surface because of their relatively high surface-area-to-volume ratios. Supportive evidence for the above can be found in the scatter diagram of Fig. 61.32, which is a plot of the average rms surface roughness values on a logarithmic scale obtained at the conclusion of each of the 27 core polishing experiments versus the difference between the fluid pH and the IEP values of the polishing agents. Each plotted symbol in Fig. 61.32 represents one polishing session for the indicated glass type and polishing agent at a given pH value. The abscissa, pH–IEP, is an opposite indicator of the sign of the surface charge on the polishing agent. Note that for pH values larger than the IEP of the polishing agent (i.e., for which the polishing agent and glass are negatively charged), the surface roughness values were, without exception, quite low. When the pH is less than the IEP, large values of roughness were observed for some combinations of polishing agent, glass type, and pH; we term this phenomenon the *slurry charge control effect.*

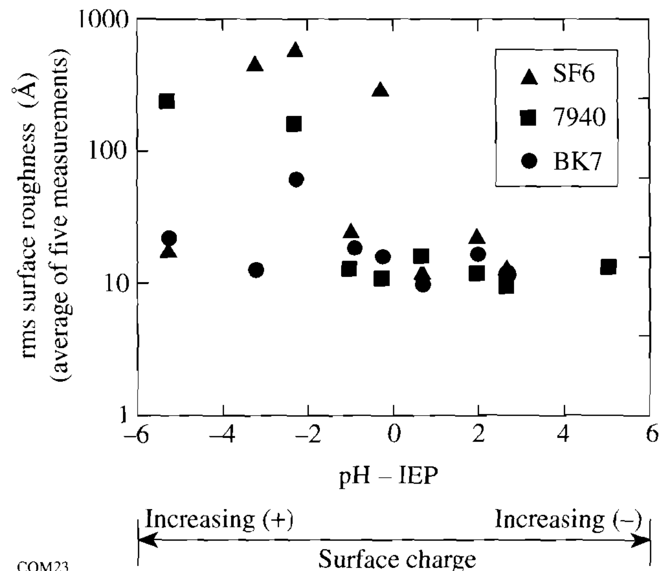

Figure 61.32
Dependence of the glass surface roughness on the difference between the fluid pH and the isoelectric point of the polishing agent (measured in 0.01-M aqueous NaCl). Each data point corresponds to a unique combination of polishing agent (CeO_2, monoclinic ZrO_2, or nanocrystalline Al_2O_3), glass type (7940, BK7, or SF6), and slurry pH (4, 7, or 10).

Interpretation of the slurry charge control effect is quite simple as summarized in Table 61.X. For glass types with a silica network, the combination of fluid and polishing agent should be selected so that the fluid pH is always larger than the IEP of the polishing agent. This precaution ensures that both the polishing agent particles and any silica species have surface charge of the same sign. As was mentioned previously, the corresponding repulsive electrostatic force inhibits agglomeration of any particles suspended in the slurry, resulting in the smoothest possible surface finishes.

Referring to Figs. 61.33 and 61.34, the polishing of 7940 with nanocrystalline Al_2O_3 provides an excellent example of the slurry charge control effect. In terms of both removal rate and surface roughness, the best results were obtained at pH 10, where both the polishing agent particles and the glass work had relatively large negative charge densities. At pH 7, where the polishing agent particles and the glass work were oppositely charged, significant agglomeration occurred, causing an increase in the surface roughness and a decrease in the removal

Table 61.X: Qualitative summary of the slurry charge control effect. *The smoothest surfaces are obtained using combinations of polishing agent and glass type with surface charge of the same sign.*

Materials	IEP	Surface Charge State at pH 4	Surface Charge State at pH 7	Surface Charge State at pH 10
Polishing Agents				
CeO_2	7.3 (a)	++	0+	–
m-ZrO_2	5.0 (a)	+	–	– –
n-Al_2O_3	9.3 (a)	++	+	–
Glass Types				
7940	3.7 (b)	0–	–	– –
BK7	3.2 (b)	–	–	– –
SF6	3.4 (b)	–	–	– –

(a) Measured in aqueous NaCl (0.01 M) using electrophoretic light scattering
(b) Measured in aqueous KCl (0.001M) using the streaming potential technique
++ Relatively large positive charge density
+ Relatively small positive charge density
0+ Slight positive charge density (pH close to the IEP)
0– Slight negative charge density (pH close to the IEP)
– Relatively small negative charge density
– – Relatively large negative charge density

rate. At pH 4, no agglomeration occurred since the polishing agent particles had a relatively high positive charge density, while the glass work had only a slight negative charge density. The removal rate in this system was nearly as high as with the pH 10 slurry. The corresponding large value of surface roughness at pH 4 is probably due to the reduced solubility of silica in the acidic environment, which inhibited corrosion of the network.

Landingham *et al.* have previously encountered agglomeration problems in the pitch polishing of fused silica with Al_2O_3.[52] In hindsight, this is not surprising since their investigation was limited to slurry pH values between 7.4 and 9.0, where silica and Al_2O_3 are oppositely charged. Although the more recent success of Tesar *et al.*[12] in the pitch polishing of fused silica with CeO_2 and monoclinic ZrO_2 at pH 4 appears to be at odds with the slurry charge control effect, their slurries were dispensed at a very low rate (1.2 ml/min.) and were not recirculated. These two process features reduced the tendency of the polishing agent to agglomerate because the accumulation of silica species in the slurry was negligible. Since no results were reported by Tesar *et al.* at pH 10, we were unable to make a more direct comparison of their results with our own.

Conclusions

The concepts and analytical tools of colloid science for characterization of surface charge effects were used in this work to demonstrate the strengths and limitations of a newly proposed polishing process rate model. The pivotal role of slurry fluid chemistry, particularly pH, in maintaining

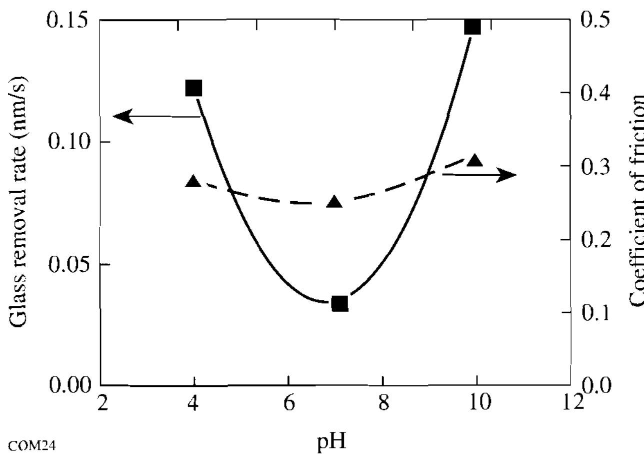

Figure 61.33
Glass removal rate and coefficient of friction between the work and the polyurethane pad as a function of slurry pH for polishing of 7940 with nanocrystalline Al_2O_3.

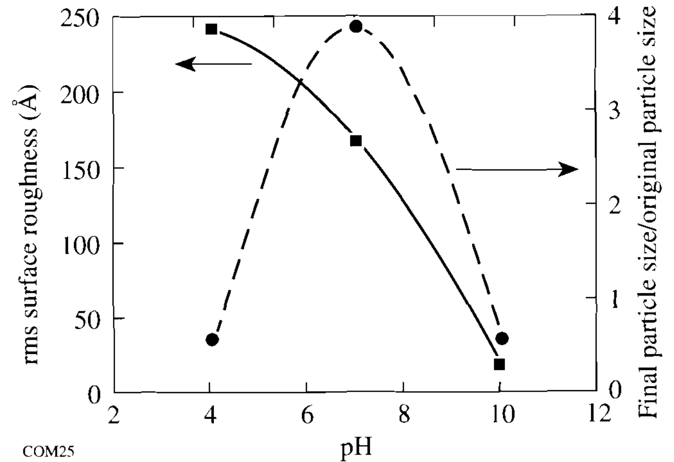

Figure 61.34
Surface roughness and the final median particle size of the slurry divided by the original median particle size as a function of slurry pH for polishing of 7940 with nanocrystalline Al_2O_3.

electrokinetically favorable conditions for a well-dispersed polishing agent was also identified and explored. For the silicate glass types studied here, these electrokinetically favorable conditions were sufficient for obtaining the smoothest possible surfaces. A relationship between fluid pH and the isoelectric point of the polishing agent, termed the slurry charge control effect, was also established, and its importance in controlling surface roughness was demonstrated. Our results have shown that there are chemically modulated forces present in the polishing system that can be equal to and, in some cases, exceed the mechanical forces and that these chemically modulated forces exert their effect at the interparticle level, not between individual particles and the glass work. The latter was most clearly demonstrated by the performance of nano-crystalline Al_2O_3, which was limited by the slurry fluid pH and not by the mechanical friability of individual polishing agent particles. The pH of the fluid and the IEP of the polishing agent were also shown to be the process parameters that, if carefully controlled, can lead to the production of higher-quality surfaces in less time.

ACKNOWLEDGMENTS

The authors extend their thanks to the following individuals and organizations for providing many helpful suggestions: T. S. Izumitani (Hoya Corporation) and L. M. Cook (Rodel Products Corp.). Glass samples were prepared under the skillful guidance of the University of Rochester's master opticians. K. H. Kubath and A. Maltsev. Generous financial support was provided by Bausch & Lomb, the Center for Optics Manufacturing (COM) through the U.S. Army Mantech Program, the New York State Center for Advanced Optical Technology (NYSCAOT), and the U.S. Department of Energy Office of Inertial Confinement Fusion under Cooperative Agreement No. DE-FC03-92SF19460.

REFERENCES

1. R. H. Doremus, *Glass Science* (Wiley, NY, 1973), Chap. 13, pp. 229–252.
2. M. J. Cumbo, "Chemo-Mechanical Interactions in Optical Polishing," Ph.D. thesis, University of Rochester, 1993.
3. T. S. Izumitani, *Optical Glass* (AIP Translation Series, NY, 1986), Chap. 4, pp. 91–146.
4. L. M. Cook, J. Non-Cryst. Solids **120**, 152 (1990).
5. F. W. Preston, J. Soc. Glass Technol. **11**, 214 (1927).
6. G. M. Sanger and S. D. Fantone, in *CRC Handbook of Laser Science and Technology*, Vol. V, Part 3, edited by M. J. Weber (CRC Press, Boca Raton, FL, 1987), pp. 461–500.
7. N. J. Brown, Lawrence Livermore National Laboratory Report MISC 4476, p. 6 (1990).
8. A. A. Tesar and B. A. Fuchs, in *Optical Fabrication and Testing Workshop*, OSA Technical Digest, Vol. 24, WB9-1 (Optical Society of America, Washington, DC, 1992), pp. 137–140.
9. A. A. Tesar and B. A. Fuchs, in *Advanced Optical Manufacturing and Testing II*, edited by V. J. Doherty (SPIE, Bellingham, WA, 1991), Vol. 1531, pp. 80–90.
10. N. J. Brown, in *Contemporary Methods in Optical Fabrication*, edited by C. L. Stonecypher (SPIE, Bellingham, WA, 1981), Vol. 306, pp. 42–57.
11. D. Golini and S. D. Jacobs, Appl. Opt. **30**, 2761 (1991).
12. A. A. Tesar, B. A. Fuchs and P. P. Hed, Appl. Opt. **31**, 7164 (1992).
13. M. J. Cumbo and S. D. Jacobs, Nanotechnology **5**, 70 (1994).
14. R. J. Hunter, *Zeta Potential in Colloid Science: Principles and Applications* (Academic Press, New York, 1981), pp. 17–18.
15. *Ibid.*, pp. 59–178.
16. D. Fairhurst and V. Ribisch, "Zeta Potential Measurements of Irregular Shape Solid Materials," in *Particle Size Distribution II*, American Chemical Society Symposium Series, No. 472, 337–353 (1991).
17. Corning 7940 fused silica, courtesy of L. Sutton, Corning Inc., Canton, NY 13617.
18. Schott BK7 (borosilicate crown) and Schott SF6 (dense flint), courtesy of A. Marker, Schott Glass Technologies Inc., Duryea, PA 18642.
19. "Corning Premium-Quality Fused Silica Low Expansion Material Code 7940," Corning Inc., Corning, NY 14830.
20. T. S. Izumitani, *Optical Glass* (AIP Translation Series, NY, 1986), p. 21.
21. Optical Glass Catalog, Schott Glass Technologies, Duryea, PA.
22. CE-RITE HP, High Purity Cerium Oxide, Code 480-G, lot # 910876, courtesy of D. Coller, Transelco Div., Ferro Corp., Penn Yan, NY 14527.
23. Zirconia Q, batch #15030492, courtesy of D. Rostoker, Saint Gobain/Norton Industrial Ceramics Corp., Worcester, MA 01615.
24. NANO-SIZE ALPHA, batch #0001-92, courtesy of D. Rostoker, Saint Gobain/Norton Industrial Ceramics Corp., Worcester, MA 01615. This is a blocky a-Al_2O_3 abrasive with individual crystallite sizes of the order of 50 nm (patent pending).
25. T. Izumitani, in *Treatise on Material Science and Technology*, edited by M. Tomozawa and R. H. Doremus (Academic, New York, 1979), Vol. 17, pp. 138–140.
26. S. D. Jacobs, "Optical Glasses and Optical Fabrication," Optics 443 course notes, University of Rochester (1994), Chap. 6, p. 11.
27. "Microgrit WCA Specifications," Micro Abrasives Corporation, Westfield, MA 01086.

28. Pocket Surf III, Federal Products Corp., Providence, RI 02905.

29. A. Lindquist, S. D. Jacobs, and A. Feltz, in *Science of Optical Finishing*, OSA Technical Digest, Vol. 9., SMC3-1 (Optical Society of America, Washington, DC, 1990), pp. 57-60. SSD measurements courtesy of T. M. Rich, Center for Optics Manufacturing, University of Rochester.

30. Brookhaven EKA, Brookhaven Instruments Corp., Holtsville, NY 11742.

31. MIL-0-13830A, Revision L, (1980).

32. Brookhaven ZetaPlus, Brookhaven Instruments Corp., Holtsville, NY 11742.

33. F. M. Ernsberger, J. Am. Ceram. Soc. **42**, 373 (1959).

34. J. Jednacak, V. Pravdic and W. Haller, J. Colloid Interface Sci. **49**, 16 (1974).

35. R. J. Hunter, *Zeta Potential in Colloid Science: Principles and Applications* (Academic Press, London, 1981), p. 249.

36. R. H. Ottewill, "Electrokinetic Properties," Fifth Annual Short Course on Colloid Science Principles & Practice, University of Massachusetts (1992), p. 7.10.

37. L. M. Cook, Rodel Products Corp., Newark, DE 19713 (personal communication, 1992).

38. Horiba LA900, Horiba Instruments Inc., Irvine, CA 92714.

39. J. S. Reed, *Introduction to the Principles of Ceramic Processing* (John Wiley & Sons, NY, 1988), pp. 90–92.

40. F. Cooke, N. Brown and E. Prochnow, Opt. Eng. **15**, 407 (1976).

41. EL Load Cell, Model #ELF-1000-100, Entran Devices, Inc., Fairfield, NJ 07004.

42. HSP, Rodel Products Corp., Scottsdale, AZ 85258.

43. J. J. Bohache, "A Study of the Optical Polishing Process," Ph.D. thesis, University of Rochester, 1978, p. 143.

44. As suggested by H. Koch, Planar Optics, Inc., Webster, NY 14580 (personal communication, 1992).

45. Zygo Maxim-3D Model 5700, Zygo Corp., Middlefield, CT 06455. Using a 20X Mirau objective, this noncontact optical profiler has a 0.1-nm vertical resolution, a field of view of 0.453×0.411 mm, and a 1.75-μm lateral resolution.

46. Davidson D305LV, Davidson Optronics Inc., West Covina, CA 91790.

47. F. K. Aleinikov, Sov. Phys.-Tech. Phy. **27**, 2529 (1957).

48. J. Jednacak, V. Pravdic, and W. Haller, J. Colloid Interface Sci. **49**, 16 (1974). The authors confined most of their study to chemically durable silica-rich glass types.

49. R. J. Hunter, *Zeta Potential in Colloid Science: Principles and Applications* (Academic Press, London, 1981), p. 233. Any ion whose adsorption at a surface is influenced by factors other than the electrical potential there (e.g., covalent bonding with surface atoms) is regarded as being specifically adsorbed.

50. J. H. Escard and D. J. Brion, J. Am. Ceram. Soc. **58**, 296 (1975).

51. R. H. Doremus, *Glass Science* (Wiley, NY, 1973), p. 243.

52. R. L. Landingham, A. W. Casey, and Roy O. Lindahl, in *The Science of Ceramic Machining and Surface Finishing II*, edited by B. J. Hockey and R. W. Rice, NBS Special Publication 562 (U.S. Government Printing Office, Washington, DC, 1979), pp. 231–245.